# LARGE EDDY SIMULATION OF A COMPRESSIBLE MIXING LAYER WITH A TIME SELF-ADAPTIVE MULTILEVEL METHOD

**Marc Terracol, Pierre Sagaut**
ONERA, 29 av. de la Division Leclerc
92320 Châtillon , France.
terracol@onera.fr, sagaut@onera.fr

**Claude Basdevant**
Université Paris-Nord, LAGA UMR 7539,
99 av. J.B. Clément, 93430 Villetaneuse, France
basdevan@ella.ens.fr

## ABSTRACT

Large-Eddy Simulation (LES) allows to reduce the computational costs in the numerical simulation of turbulent flows in comparison with Direct Numerical Simulation (DNS). This reduction is obtained by a scale separation, the largest ones being directly resolved, while the smallest ones (subgrid scales) are modeled. Nevertheless, usual eddy-viscosity subgrid models have been developed in the framework of homogeneous isotropic turbulence, and are so not able to take into account in a proper way the presence of inhomogeneous subgrid scales, or backscatter. That is why LES still require the use of fine computational grids, and thus a large amount of CPU ressources. A multilevel method applied to LES is introduced here to reduce the CPU times. Flow variables are decomposed into several frequency bands, each band being associated to a computational grid in physical space. The high-frequency deterministic information from the finest levels can then directly be used on the coarse ones to get an accurate evaluation of the subgrid model, as in deconvolution-like approaches (Stoltz and Adams, 1999, Domaradzki and Yee, 2000). CPU time saving is obtained by performing the main part of the simulation on the coarse levels by freezing the smallest resolved scales (Quasi-Static approximation - Dubois *et al.*, 1998), and performing an explicit reconstruction of these scales at certain times only. Such a strategy has previously been assessed on a quasi-steady plane channel flow configuration (Terracol *et al.*, 2001a) by the use of a simple V-cycling strategy. Here, a particular two-level case of this method is considered for fully unsteady flows, in which a dynamic evaluation of the time during which the QS approximation remains valid is performed by a priori estimates of the small scales time variation. The method is assessed here on a fully unsteady time-developing compressible mixing layer.

## MULTILEVEL DECOMPOSITION

We consider the framework of a multilevel decomposition of any variable $\phi$ of the flow by the use of $N$ different filtering levels. Each level is defined by mean of a family of low-pass filters $\{G_n\}$, $n \in [1, N]$ which are characterized by their cutoff lenghtscales $\Delta_n$, associated to the cutoff wave numbers $k_n$ in spectral space. Any filtered variable is then formally defined as the convolution product of the continuous variable with the filter kernel $G_n$ :

$$G_n \star \phi(x,t) = \int_\Omega G_n(x-\xi)\phi(\xi,t)d\xi \qquad (1)$$

where $x \in \Omega \subset \mathbb{R}^3$ is the space coordinates vector, and $t \in \mathbb{R}^+$ is time.
Hereafter, the case $\Delta_{n+1} \geq 2\Delta_n$ will be considered, or equivalently $k_{n+1} \leq k_n/2$.
The filtered variables at the finest level of resolution are defined as $\overline{\phi}^{(1)} = G_1 \star \phi$.
The filtered variables at the level $n \in [2, N]$ are then recursively defined as :

$$\begin{aligned} \overline{\phi}^{(n)} &= G_n \star G_{n-1} \star ... \star G_2 \star G_1 \star \phi \\ &= \mathcal{G}_1^n(\phi) \end{aligned} \qquad (2)$$

with, for any $m \in [1, n]$: $\mathcal{G}_m^n(.) = G_n \star G_{n-1} \star ...G_{m+1} \star G_m \star (.)$ . Each flow variable $\phi$ can then be decomposed as :

$$\phi = \overline{\phi}^{(n)} + \sum_{l=1}^{n-1} \delta\phi^l + \phi" \qquad (3)$$

where: $\overline{\phi}^{(n)} = \mathcal{G}_1^n(\phi)$, $\delta\phi^l = \overline{\phi}^{(l)} - \overline{\phi}^{(l+1)}$, and $\phi" = \phi - \overline{\phi}^{(1)} = \delta\phi^0$. In the compressible case, density-weighted filtering is used.

In the multilevel decomposition (3), $\overline{\phi}^{(n)}$ corresponds to the resolved scales at the $n$th level of resolution. The details $\delta\phi^l$ correspond to the scales resolved at the level $l$, which are unresolved at the level $l+1$, and $\phi"$ corresponds to the finest level unresolved scales. For $N = 1$, the classical LES decomposition is obtained.

## BASIC EQUATIONS

We consider the dimensionless compressible Navier-Stokes equations :

$$\frac{\partial V}{\partial t} + \mathcal{N}(V) = 0 \tag{4}$$

where $V = \left(\rho, \rho U^T, \rho E\right)^T$, $U = (u_1, u_2, u_3)^T$ and :

$$\mathcal{N}(V) = \begin{pmatrix} \nabla.(\rho U) \\ \nabla.(\rho U \otimes U) + \nabla p - \nabla.\sigma \\ \nabla.\left((\rho E + p)U\right) - \nabla.(\sigma : U) + \nabla.Q \end{pmatrix}$$

where $p$ is the pressure, $\rho$ the density, $U$ the velocity vector, and $\rho E$ the total energy. Classical expressions are used for the viscous stress tensor $\sigma$ and viscous heat flux vector $Q$.

The filtered equations at any level $n \in [1, N]$ are simply obtained by applying the filtering operator $\mathcal{G}_1^n$ to equation (4). Assuming classicaly commutation of the filtering operation with time derivatives, the filtered equations at the level $n$ are :

$$\frac{\partial \overline{V}^{(n)}}{\partial t} + \mathcal{N}\left(\overline{V}^{(n)}\right) = -\mathcal{T}^{(n)} \tag{5}$$

where $\mathcal{T}^{(n)}$ is the subgrid term defined as :

$$\begin{aligned} \mathcal{T}^{(n)} &= \overline{\mathcal{N}(V)}^{(n)} - \mathcal{N}\left(\overline{V}^{(n)}\right) \\ &= [\mathcal{G}_1^n, \mathcal{N}](V) \end{aligned} \tag{6}$$

The commutator [., .] takes into account all the commutation errors between two operators :

$$[\mathcal{F}, \mathcal{G}] = \mathcal{F}_\circ\mathcal{G} - \mathcal{G}_\circ\mathcal{F}$$

Commutation errors between space derivatives and filters are included in $\mathcal{T}^{(n)}$. However, if the filters used are commutative with space derivatives, the only remaining term in $\mathcal{T}^{(n)}$ comes from the non-linear (convective) term.

## MULTILEVEL SUBGRID CLOSURE

At each resolution level $n$, the subgrid term $\mathcal{T}^{(n)}$ requires a closure because $\overline{\mathcal{N}(V)}^{(n)}$ remains uncomputable. By reccurence, the following relation is obtained :

$$\begin{aligned} \mathcal{T}^{(n)} &= [\mathcal{G}_1^n, \mathcal{N}](V) \\ &= \sum_{l=1}^{n-1} [\mathcal{G}_{l+1}^n \star, \mathcal{N}](\overline{V}^{(l)}) + \mathcal{G}_2^n\left(\mathcal{T}^{(1)}\right) \end{aligned} \tag{7}$$

In this relation, the only term that needs to be parametrized is $\mathcal{T}^{(1)}$, corresponding to interactions with the unresolved scales from the finest level. Provided that $k_1$ is sufficiently large, a simple LES closure (see Sagaut, 2001 for a review) can be used to compute $\mathcal{T}^{(1)}$. On the coarser levels, the subgrid terms can then be simply evaluated by relation (7). Notice that in this general relation, no assumption about commutativity of the filtering operations with space derivatives is used. This last point can be of great interest for applications using non-uniform meshes where commutation errors may occur. Moreover, all the non-linearities are taken into account, while classical closures neglect the subgrid terms associated to the non-linear expressions of the viscous terms $\sigma$ and $Q$. Finally, no particular form of the subgrid term is assumed: both the dissipative forward transfer and the anti-dissipative backscatter of energy are represented, while traditional eddy-viscosity models are strictly dissipative .

Relation (7) can also be interpreted as a $N$-level generalization of the well-known Germano's identity (Germano, 1986). In particular, it can simply be re-written as :

$$\mathcal{T}^{(n+1)} - G_{n+1} \star \mathcal{T}^{(n)} = [G_{n+1}\star, \mathcal{N}](\overline{V}^{(n)}) \tag{8}$$

which falls into the original Germano's identity when $n = 1$ and when commutativity of the filters with space derivatives is assumed (*i.e.* $[G_n\star, \nabla] = 0$).

## TIME SELF-ADAPTIVE PROCEDURE

### Discrete multilevel formalism

From a practical point of view, the finest filtering level is implicitely defined by the space discretization, as it is generally the case in Large-Eddy Simulation. The multilevel scale separation is then obtained through the use of a hierarchy of embedded grids, as it was already the case in Terracol *et al.*(2001a). For

any field $\overline{\phi}^{(n)}$ on the $n$-th grid level, the field $\overline{\phi}^{(n+1)}$ on the coarser grid level corresponding to the $(n+1)$-th filtering level is given by $\overline{\phi}^{(n+1)} = R_n^{n+1}(\overline{\phi}^{(n)})$, where $R_n^{n+1}$ is a fine-to-coarse interpolation operator acting as a discrete filter on the solution. The frequency complement $\delta\phi^n$ between the two levels $n$ and $n+1$ is simply given on the $n$-th grid level by: $\delta\phi^n = \overline{\phi}^{(n)} - P_{n+1}^n(\overline{\phi}^{(n+1)}) = (Id^n - P_{n+1} \circ R_n^{n+1})(\overline{\phi}^{(n)})$, where $P_n^{n+1}$ is a coarse-to-fine interpolation operator. This leads to a simple exact reconstruction of $\overline{\phi}^{(n)}$ from $\overline{\phi}^{(n+1)}$ and $\delta\phi^n$ by: $\overline{\phi}^{(n)} = P_{n+1}^n(\overline{\phi}^{(n+1)}) + \delta\phi^n$.

This hierarchy of $N$ embedded grids realises a $N$-level multilevel decomposition of the flow, in which each continuous filtering operator $G_n$ is formally equivalent to the discrete one $R_{n-1}^n$, and each level cut-off number $k_n$ is implicitely defined by $R_{n-1}^n$ and by the numerical cut-off wave number of the grid $n$.

### Time-adaptive multigrid cycling procedure

In the present paper, a simple two-level V-cycling strategy in time has been retained. It is an extension of the one used in steady multigrid algorithms. For $N = 2$, one cycle is defined as follows :

**i** - Starting from time $t_0$, any variable $\overline{\phi}^{(1)}$ from the fine grid is restricted on the second grid by the use of the restriction operator $R_1^2$, while the associated frequency complement $\delta\phi^1 = \overline{\phi}^{(1)} - P_2^1(\overline{\phi}^{(2)})$ is stored on the fine grid.

**ii** - Time integration is then performed on the coarse grid with the multilevel closure (7) during $N_c$ time steps satisfying the CFL condition on the second grid. The second grid being defined from the fine one by keeping half the number of mesh points in each direction, the time step on this grid is twice the fine grid's one: $2\Delta t$.

**iii** - After time integration on the coarse grid $(t = t_0 + 2N_c\Delta t)$, the resulting field is interpolated to the fine grid by the use of the interpolation operator $P_2^1$. The correct frequential level on the fine grid is then obtained by adding to the interpolated low-frequency field the frequency complement $\delta\phi^1$ kept frozen during the coarse level time integration :

$$\overline{\phi}^{(1)}(t_0 + 2N_c\Delta t) = P_2^1(\overline{\phi}^{(2)}(t_0 + 2N_c\Delta t)) + \delta\phi^1(t_0) \quad (9)$$

**iv** - The small scales are then refreshed and recorrelated to the large-scale field by proceeding to time integration of the whole high-frequency field with a standard LES closure on the fine grid level during one time step $\Delta t$. The new fine-level field $\overline{\phi}^{(1)}(t_0 + (1 + 2N_c)\Delta t)$ will then be used to compute the closure terms on the coarse grid during the next cycle.

A similar strategy is used in the extension of the velocity estimation model of Domaradzki and Yee (2000) to high Reynolds numbers, where an integration of the full Navier-Stokes equations is performed on a two times finer computational grid to regenerate small scales. While this cycling strategy is unconsistent in time, it can be used for unsteady simulations provided the QS approximation (Dubois *et al.*, 1998) is satisfied. That is to say that the time variation of the frequency complement $\delta\phi^1$ of any variable $\phi$ can be neglected during the time integration on the coarse grid. Indeed, Dubois *et al.*(1998) have shown that the smallest scales of the flow require less accuracy in time than the large energy-containing ones because they reach equilibrium more quickly.

The originality of the present approach is to proceed dynamically to an estimation of the time during which the QS approximation remains valid and coarse-grid time integration is allowed. This is achieved by the use of a parameter $\varepsilon_{max}$ which represents the maximum value allowed for the relative variation of the total energy associated to the small scales in the range $k_2 < k < k_1$. The number of time steps $N_c$ allowed on the coarse grid is then evaluated at each fine-to-coarse restriction step such that :

$$2N_c\Delta t \left\| \frac{\partial}{\partial t}\delta e^{(1)} \right\|_2 / \left\| \widehat{\rho E}^{(1)} \right\|_2 < \varepsilon_{max} \quad (10)$$

where $\widehat{\rho E}^{(n)}$ is the resolved energy at level $n$, $\delta e^{(1)} = \widehat{\rho E}^{(1)} - P_2^1(\widehat{\rho E}^{(2)})$, and $\|.\|_2$ is the $\mathcal{L}_2$-norm. The time derivative in (10) is simply evaluated by a backward first-order approximation. The parameter $\varepsilon_{max}$ is directly linked to the error commited on the smallest scales of the flow, and should then be chosen to avoid a too important time decorrelation between large and small scales, which can lead to numerical instabilities.

## APPLICATION: COMPRESSIBLE MIXING LAYER

The proposed algorithm has been applied to the case of a time-developing compressible mix-

ing layer (Vreman *et al.*, 1997, Comte *et al.*, 1992, Moser and Rogers, 1991). This flow is a typical example of a fully unsteady case, in which different scales, both in space and time are present.

### Numerical scheme

The numerical scheme used is a classical cell-centered finite-volume scheme, in which the convective fluxes are evaluated under their skew-symmetric form (see Ducros *et al.*, 1999) to reduce aliasing errors, and the viscous ones using a staggered formulation. The time integration is performed using a third-order low-storage Runge-Kutta scheme (see Lenormand *et al.*, 2000). This leads to a non-dissipative scheme which is second-order accurate in space, and third-order accurate in time. Finally, the grid transfer operators used in all the multilevel simulations are third-order accurate non-dissipative operators.

### Computational cases

The computational domain is a rectangular box $[0; L_x] \times [-L_y/2; L_y/2] \times [0; L_z]$, with periodic boundary conditions in the streamwise ($x$) and spanwise ($z$) directions, and an outflow condition in the normal ($y$) direction.

As in Vreman *et al.*(1997), the flow is initiated by an hyperbolic-tangent-law profile for the streamwise velocity component :

$$u_1(y, t = 0) = U_\infty \tanh(\frac{2y}{\delta_0}) \qquad (11)$$

where $U_\infty = 1$ and $\delta_0 = 1/7N_{rol}$ is the initial vorticity thickness, with $N_{rol}$ the number of primary rollers of the simulation. The initial mean density is uniform ($\rho = 1$), and the mean temperature is given by the Busemann-Crocco law (Ragab and Wu, 1989). Two types of computations have been carried out, corresponding to two different values of $Re_{\delta_0}$, which is the Reynolds number based on the upper velocity $U_\infty$, and on the initial vorticity thickness $\delta_0$. The simulation Mach number is $M = 0.2$. All the simulations reported here have been performed with an eddy-viscosity Smagorinsky model (see Sagaut, 2001) at the finest level of resolution, where the Smagorinsky constant is set to $C_s = 0.18$, while the multilevel subgrid closure is used on the coarse level in the two-level simulations.

For both the two Reynolds cases, several two-level simulations, corresponding to different values of the parameter $\varepsilon_{max}$ have been carried out, and compared to a fine monolevel simulation, used as reference in our study. A coarse monolevel run has been carried out too, and also a two-level simulation with $N_c$ fixed to one, referred to as "MG" in the folllowing.

**Low-Reynolds case:** $Re_{\delta_0} = 100$

The aim of this case, with $N_{rol} = 4$, is to assess the time-adaptive cycling strategy. Indeed, at this low Reynolds number, the effects of the subgrid model remain moderate. To initiate the primary rollers and the pairings, a two-dimensional deterministic perturbation, corresponding to the most amplified wavelength given by linear stability analysis, and a uniform white-noise are added to the mean profiles in the initial rotational zone. In this case, levels 1 and 2 correspond to two uniform grids of resolution $64^3$ and $32^3$ respectively, with $L_x = L_y = L_z = 1$. The computations are performed, from $t = 0$ to $t = 100$, with $t$ the time scaled with $U_\infty$ and $\delta_0$, leading to the occurence of two successive pairings of the rollers.

First, the influence of $\varepsilon_{max}$ has been analized through the time-averaged $\mathcal{L}_2$-norm of the relative error commited on momentum thickness $\delta_m$ of the mixing layer for several values of $\varepsilon_{max}$ taken in the range $[10^{-5}; 10^{-2}]$. From these first results, it seems that $\varepsilon_{max}$ should be taken in the range $[5.10^{-5}; 10^{-3}]$ which lead to CPU gain factors up to more than 4, with relative errors on $\delta_m$ remaining lower than 5 %.

From a phenomenological point of view, it should be mentionned that all the two-level simulations exhibit the same physical behavior than the reference fine monolevel one, with two pairings occuring around $t \simeq 50$ and $t \simeq 75$, while the coarse-grid simulation has still not undergone the second pairing at $t = 100$. The good agreement between the two-level simulations and the reference one is illustrated in Figs. 1 and 2 presenting respectively the temporal evolution of the momentum thickness $\delta_m$, and the mean streamwise velocity profile after the second pairing ($t = 90$). The same quality of results is obtained for all the aerodynamics quantities, and RMS fluctuations, at any time of the simulation. It should be mentionned that the two-level runs considered here "MG", $\varepsilon_{max} = 5 \times 10^{-5}$, and $\varepsilon_{max} = 10^{-3}$ are associated to CPU gain factors of 1.7, 1.8, and 4.15 respectively, while the results remain in very good agreement with the reference simulation.

**High-Reynolds case:** $Re_{\delta_0} = 10^{10}$

In this quasi-inviscid case, the ability of the

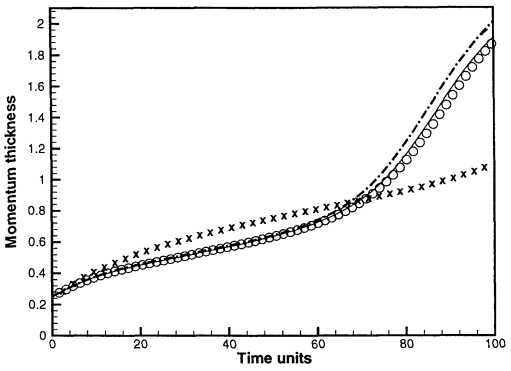


Figure 1: Momentum thickness $\delta_m$. × : Coarse monolevel, O : Fine monolevel, - - - : MG($N_c$ = 1), —— : $\varepsilon_{max} = 5 \times 10^{-5}$, -·-·- : $\varepsilon_{max} = 1 \times 10^{-3}$

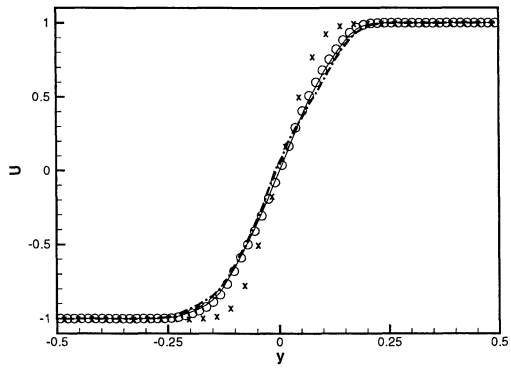


Figure 2: Low $Re$ case: streamwise velocity profile, $t$=90 (See Fig. 1 for caption).

multilevel closure of dealing with highly turbulent flows is studied, since in this case, the only dissipation present in the simulation is related to the subgrid model used.

Here, the case $N_{rol} = 8$ in a computational box of dimensions $L_x = 1$, $L_y = 40\delta_0$, and $L_z = \frac{2}{3}L_x$ is considered. The resolution of the fine grid is $120 \times 100 \times 60$. The grid is uniform in the streamwise and spanwise directions, while it is refined in the shear layer of the flow $[-L_y/8; L_y/8]$. The coarse grid is defined from the fine one, by keeping half the number of points in each direction, yielding to the definition of a $60 \times 50 \times 30$ grid. To initiate the pairings, only a white noise perturbation is added to the initial mean profiles.

The simulations have been performed from $t = 0$ to $t = 160$, and exhibit the same physical behavior, except the coarse LES which is less turbulent, and remains quasi-bidimensional. That can be explained by an over-dissipative behavior of the model with the coarse resolution, preventing the development of transverse modes. On the other hand, all the other simulations exhibit the same strongly turbulent and three-dimensional behavior, with the presence of helicoïdal pairings, as mentionned by Comte *et al.*(1992). The resulting vortex-lattice structure at $t = 60$ is illustrated by an iso-Q levels visualization (Hunt *et al.*, 1988) in Fig. 3.

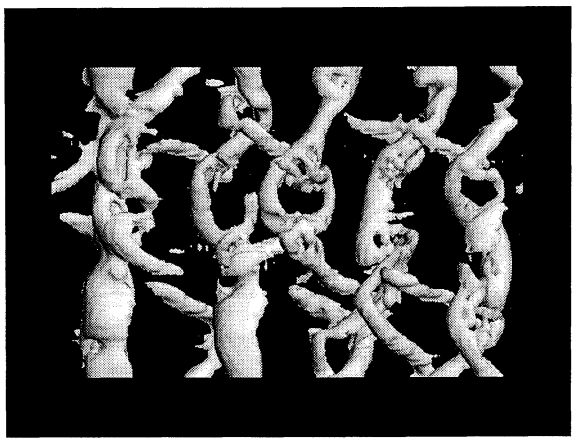

Figure 3: Helicoïdal pairing : top view of iso-Q surfaces at t=60

After $t \simeq 100$, a small-scale transition occurs, resulting in a sudden loss of kinetic energy and the establishment of a Kolmogorov-like spectrum. This point is illustrated by Figs. 4 and 5 presenting respectively the time decrease of kinetic energy and the mono-dimensional streamwise energy spectra obtained at $t = 160$ for each of the computational cases considered: fine monolevel, "MG", $\varepsilon_{max} = 10^{-4}$, $\varepsilon_{max} = 10^{-3}$, and coarse-grid computation. Again, a very good agreement is observed between all the two-level runs and the reference simulation.

It appears that no small-scale transition occurs in the coarse-grid simulation since no sudden decrease of kinetic energy is observed on Fig. 4. This is also confirmed by three-dimensional visualizations of the flow, and by Fig. 5. On the other hand, all the two-level computations "MG", $\varepsilon_{max} = 10^{-4}$, $\varepsilon_{max} = 10^{-3}$, corresponding to CPU gain factors of 1.8, 1.97, and 3.5, exhibit the good physical behavior, and are in very good agreement with the reference simulation. It also appears that even the highest frequencies are well-resolved, despite the QS approximation.

The good agreement between the multilevel computations and the reference ones is also illustrated by Fig. 6 presenting the mean streamwise velocity profiles at $t = 100$, while the same quality of results is obtained again

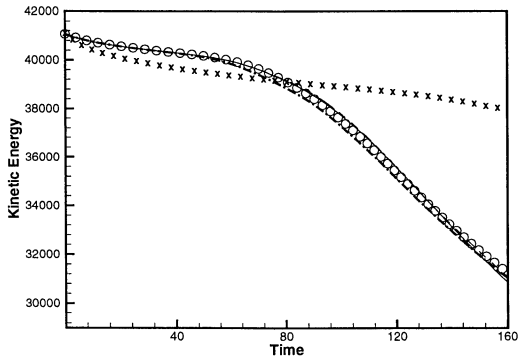


Figure 4: Total kinetic energy. × : Coarse monolevel, ○ : Fine monolevel, – – – : MG($N_c$ = 1), —— : $\varepsilon_{max} = 1 \times 10^{-4}$, -·-·- : $\varepsilon_{max} = 1 \times 10^{-3}$

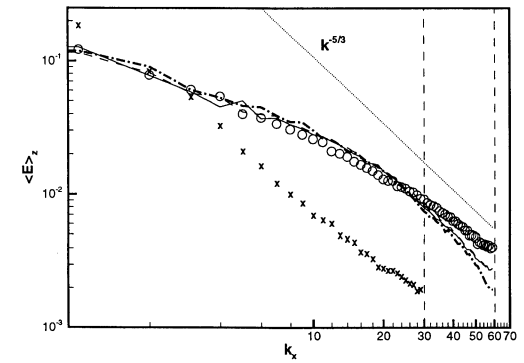


Figure 5: Streamwise energy spectrum at $t = 160$ (See Fig. 4 for caption).

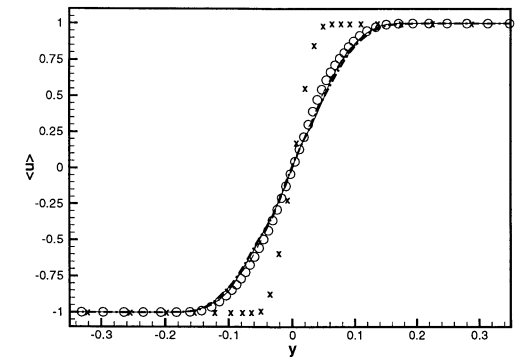


Figure 6: High $Re$ case: streamwise velocity profile, $t$=100 (See Fig. 4 for caption).

for other quantities as RMS fluctuations.

Finally, it should be mentionned that all the simulations, except the coarse-grid one, exhibit a self-similar phase between the second and third pairings, as it should be the case in high Reynolds number mixing layer (Vreman *et al.*, 1997).

## CONCLUSION

A two-level methodology to perform LES at lower cost has been presented and assessed in a time-developing mixing layer configuration, for both a low and a high value of the Reynolds number. It results that the multilevel closure proposed is very efficient, and allows to get results in good agreement with fine monolevel LES. Moreover, it was shown in a more detailled study (Terracol *et al.*, 2001b) that this closure is able to deal with backward transfer of energy. The time self-adaptive procedure allows to improve the results in comparison with non-adaptive multilevel computations, while the simulation times are significantly reduced by a factor between two and four in comparison with standard LES.

## REFERENCES

P. Comte, M. Lesieur, and E. Lamballais. Large- and small-scale stirring of vorticity and a passive scalar in a 3-D temporal mixing layer. *Phys. Fluids A*, 4(12):2761–2778, 1992.

J.A. Domaradzki and P.P. Yee. The subgrid-scale estimation model for high Reynolds number turbulence. *Phys. Fluids*, 12(1):193–196, 2000.

T. Dubois, F. Jauberteau, and R. Temam. Incremental unknowns, multilevel methods and the numerical simulation of turbulence. *Comput. Methods Appl. Mech. Engrg.*, 159:123–189, 1998.

F. Ducros, V. Ferrand, F. Nicoud, C. Weber, D. Darracq, C. Gacherrieu, and T. Poinsot. Large-Eddy Simulation of the shock-turbulence interaction. *J. Comput. Phys.*, 152(2):517–549, 1999.

M. Germano. A proposal for a redefinition of the turbulent stresses in the filtered Navier-Stokes equations. *Phys. Fluids*, 29(7):2323–2324, 1986.

J. C. R. Hunt, A. A. Wray, and P. Moin. Eddies, stream, and convergence zones in turbulent flows. *Technical Report CTR-S88, Center for Turbulence Research*, 1988.

E. Lenormand, P. Sagaut, and L. Ta Phuoc. Large-Eddy Simulation of compressible channel flow at moderate Reynolds number. *Int. J. Numer. Methods Fluids*, 32:369–406, 2000.

R. D. Moser and M. M. Rogers. Mixing transition and the cascade to small scales in a plane mixing layer. *Phys. Fluids A*, 3(5):1128–1134, 1991.

S. A. Ragab and J. L. Wu. Linear instabilities in two-dimensional compressible mixing layers. *Phys. Fluids A*, 1:957–966, 1989.

P. Sagaut. *Large-Eddy Simulation for incompressible flows*. Scientific Computation. Springer Verlag, Berlin, 2001.

S. Stolz and N.A. Adams. An approximate deconvolution procedure for large-eddy simulation. *Phys. Fluids*, 11(7):1699–1701, 1999.

M. Terracol, P. Sagaut, and C. Basdevant. A multilevel algorithm for Large Eddy Simulation of turbulent compressible flows. to appear in J. Comput. Phys., 167(2), 2001a.

M. Terracol, P. Sagaut, and C. Basdevant. A time self-adaptive multiresolution algorithm for large-eddy simulation, with application to the compressible mixing layer. *Phys. Fluids*, submitted, 2001b.

B. Vreman, B. Geurts, and H. Kuerten. Large-eddy simulation of the turbulent mixing layer. *J. Fluid Mech.*, 339:357–390, 1997.